

MASTER

THE BETA-GAMMA CIRCULAR POLARIZATION
CORRELATION AND NUCLEAR MATRIX ELEMENTS OF As^{76} †

H. A. Smith* and P. C. Simms

ABSTRACT

The β - γ circular polarization correlation P_{γ} for the 2.41 MeV β transition of As^{76} has been measured as an average value over the energy interval $E_{\beta} = 1.4$ to 2.0 MeV at an average angle $\theta_{\beta\gamma} = 158$ degrees. Previous experimental data, this new value for P_{γ} , and theoretical arguments are used to set limits on the nuclear matrix elements and to investigate the diagonality of the Coulomb hamiltonian. The analysis shows that matrix elements which change the angular momentum by 0, 1, and 2 units all contribute with approximately equal strength to the transition. The matrix element analysis indicates that the A_3 term in P_{γ} is negligible compared to the A_1 term. When A_3 is set equal to zero, the experimental data gives the following value for P_{γ} :

$$P_{\gamma}(1.4 \text{ MeV} < E_{\beta} < 2.0 \text{ MeV}, \theta_{\beta\gamma} = 180^{\circ}) = 0.105 \pm 0.02$$

This report was prepared as an account of work sponsored by the United States Government. Neither the United States nor the United States Atomic Energy Commission, nor any of their employees, nor any of their contractors, subcontractors, or their employees, makes any warranty, express or implied, or assumes any legal liability or responsibility for the accuracy, completeness or usefulness of any information, apparatus, product or process disclosed, or represents that its use would not infringe privately owned rights.

DISTRIBUTION OF THIS DOCUMENT IS UNLIMITED

DISCLAIMER

This report was prepared as an account of work sponsored by an agency of the United States Government. Neither the United States Government nor any agency Thereof, nor any of their employees, makes any warranty, express or implied, or assumes any legal liability or responsibility for the accuracy, completeness, or usefulness of any information, apparatus, product, or process disclosed, or represents that its use would not infringe privately owned rights. Reference herein to any specific commercial product, process, or service by trade name, trademark, manufacturer, or otherwise does not necessarily constitute or imply its endorsement, recommendation, or favoring by the United States Government or any agency thereof. The views and opinions of authors expressed herein do not necessarily state or reflect those of the United States Government or any agency thereof.

DISCLAIMER

Portions of this document may be illegible in electronic image products. Images are produced from the best available original document.

I. INTRODUCTION

There are six nuclear matrix elements which are usually dominant in first forbidden beta transitions. In addition finite nuclear size effects give rise to higher order matrix elements other than those arising from higher forbiddenness.^{1,2} In order to extract even the six primary matrix elements, it is usually necessary to measure several of the observables associated with the transition under study. In spite of this complexity, the possibility of experimentally measuring the matrix elements of so many operators between the same two nuclear states makes first forbidden β transitions particularly attractive in nuclear structure studies.

The existing data on the 2.41-MeV β transition in As^{76} , exclusive of the β - γ circular polarization correlation P_{γ} , is not sufficient to determine the nuclear matrix elements. If, in addition to the existing data, the β - γ circular polarization correlation measured here is imposed, it is possible to establish meaningful limits on the nuclear matrix elements.

The conserved vector current (CVC) theory can be applied to first-forbidden β decay to predict the ratio of two of the vector-type matrix elements. If the calculations of Fujita³ and Eichler⁴ are used, the result is:

$$\frac{\int \vec{\alpha}}{\int i \frac{r}{\rho}} = \Lambda_{\text{CVC}}^0 \equiv (W_0 \mp 2.5)\rho \pm 1.2 \alpha Z \quad (1)$$

for β^{\mp} decay. W_0 is the β transition energy; ρ and Z are the radius

and charge of the daughter nucleus. Natural units (i.e., $\hbar = c = m_e = 1$) are used. Fujita and Eichler assumed that the off diagonal elements of the nuclear Coulomb hamiltonian could be neglected.

The more general approach of Damgaard and Winther⁵ to the vector matrix element ratio does not rely upon this approximation. Instead, a realistic form for the Coulomb potential is proposed which leads to the following prediction for the vector matrix element ratio:

$$\begin{aligned} \frac{\int \alpha}{\int_i \frac{\vec{r}}{\rho}} &= \Lambda_{CVC} \equiv (W_0 \mp 2.5)\rho \pm \frac{\alpha Z}{2}(3-\lambda) \\ &= \Lambda_{CVC}^0 \pm \frac{\alpha Z}{2}(0.6-\lambda) \end{aligned} \quad (2)$$

The parameter λ is the ratio of a higher-order matrix element to a first order matrix element:

$$\lambda = \frac{\int_i \frac{\vec{r}}{\rho} \left(\frac{\vec{r}}{\rho}\right)^2}{\int_i \frac{\vec{r}}{\rho}} \quad (3)$$

The correction term in equation 2 can be expressed in the following form:

$$\begin{aligned} \frac{\alpha Z}{2}(0.6-\lambda) &= \left\{ \sum_{f' \neq f} \langle f | H_c | f' \rangle \langle f' | i\vec{r} | i \rangle \right. \\ &\quad \left. - \sum_{i' \neq i} \langle f | i\vec{r} | i' \rangle \langle i' | H_c | i \rangle \right\} \left(\langle f | i\frac{\vec{r}}{\rho} | i \rangle \right)^{-1} \end{aligned} \quad (4)$$

The final state $|f\rangle$ and the initial state $|i\rangle$ of the β transition are members of the complete set of states $|f'\rangle$ and $|i'\rangle$, respectively.

If the off diagonal matrix elements of the Coulomb hamiltonian $\langle f|H_c|f'\rangle$ and $\langle i'|H_c|i\rangle$ are very small, the correction term can be neglected.

It is clear from equation 4 that λ will be approximately 0.6 when the contribution of the off diagonal elements of H_c is small. A complete discussion of the formulas for Λ_{CVC} and Λ_{CVC}^0 can be found in reference 6.

The β - γ angular correlation function for first-forbidden β transitions has the following form:

$$N(W, \theta, S) = A_0(W) + SA_1(W) P_1(\theta) + A_2(W) P_2(\theta) + SA_3(W) P_3(\theta) \quad (5)$$

W is the total energy of the β particle, and θ is the angle between the directions of emission of the β particle and gamma ray. The helicity factor, S , is +1 (-1) for right- (left-) circularly polarized photons. The coefficients $A_n(W)$ depend upon the nuclear matrix elements of the β transition, and $P_n(\theta)$ are the Legendre polynomials.

The β - γ circular polarization correlation is given by:

$$P_\gamma(W, \theta) = \frac{N(W, \theta, +1) - N(W, \theta, -1)}{N(W, \theta, +1) + N(W, \theta, -1)} \quad (6)$$

which with Equation (5) reduces to

$$P_\gamma(W, \theta) = \frac{A_1(W) P_1(\theta) + A_3(W) P_3(\theta)}{A_0(W) + A_2(W) P_2(\theta)} \quad (7)$$

The β - γ circular polarization correlation was measured by the method of forward Compton scattering of the photons off polarized electrons in magnetized iron. It can be shown^{7,8} that the observed circular polarization effect is given by

$$\delta = 2 \frac{C_+ - C_-}{C_+ + C_-} \quad (8)$$

when C_+ and C_- are the true β - γ coincidence counting rates for two directions of the spin of the scattering electrons. The observed effect δ can be expressed in terms of the unknown parameters $A_n(W)$ in the following way:

$$\delta = \frac{\epsilon_1 A_1(W) + \epsilon_3 A_3(W)}{A_0(W) + \epsilon_2 A_2(W)} \quad (9)$$

The parameters ϵ_n are obtained by numerical integration over the geometry of the experiment. Solid angle corrections, average values for P_n , and the circular polarization analyzer efficiency are all combined in ϵ_n . In order to determine P_γ from δ , the relative size of A_1 to A_3 and A_0 to A_2 must be known.

II. EXPERIMENTAL PROCEDURE

The geometry of the coincidence counting and scattering apparatus was such that the average angle between the gamma radiation and the symmetry axis of the β detector was 158 degrees. (See Figure 1 for a schematic diagram of the experimental apparatus.) The equipment consisted of the circular polarization analyzer magnet, the source chamber,

the β - and γ -detectors, the electronics necessary to analyze and store the data, and an automatic counting and control system used to regulate the gathering of the data.

The construction and operation of the cylindrical scattering magnet have been discussed by Alexander⁹. Detailed discussions of the rest of the experimental apparatus have been presented by Ohlms, Bosken and Simms¹⁰. Certain improvements which have been made in the instrument for the present measurement will be discussed below.

The photomultiplier tubes in the γ - and β -detectors had to be stabilized against gain shifts due to variations in counting rate and magnetic field directions. This was accomplished with two Cosmic Spectrastats (Model 1001, Cosmic Radiation Laboratory; Bellport, N.Y.) which controlled the voltage on the photomultiplier tubes. The tube voltages were varied so that a standard peak which the Spectrastat viewed remained at a constant voltage during the experiment.

The stabilizing peak on the γ side was the 122-keV γ ray following the decay of Co^{57} . The Co^{57} source was attached directly to the γ detector. The stabilizing peak on the β side was obtained by placing a small ($\frac{1}{2}$ " X $\frac{1}{2}$ ") crystal of NaI(Tl) doped with Am^{241} (an α -emitter) in the light path from the plastic scintillator to the photocathode. This "light pulser" provided a standard amount of light to the photomultiplier tube independent of the identity of the source in the β chamber. Previously this pulser had been faced away from the photomultiplier tube in order to more fully diffuse its light and uniformly illuminate the photocathode. Much of the pulser's light was lost in this way, making the effective energy of the stabilizing peak approximately 2 MeV.

In order to study high-energy β decays it was necessary to increase the effective energy of the pulser peak so that the pulser would be easy to distinguish. This was accomplished by facing the NaI(Tl) can toward the photomultiplier tube and using a light pipe between the pulser and the photocathode. In this way the effective energy of the pulser peak was increased to approximately 10 MeV, well above any β spectra of interest. In addition, β particle energy resolution did not suffer in this new configuration, as long as the usual precautions were taken to minimize light loss.

The photomultiplier tube on the β side had formerly been placed inside the source chamber¹⁰. The source chamber was shielded from the magnet by large sheets of Netic and Co-Netic metal. On both the β and γ detectors the electronic timing signals were taken from the anodes of the photomultiplier tubes, while the linear signals for energy analysis were taken from lower dynodes. Even though the influence of the changing magnetic field on the dynode signals was negligible, there was a systematic magnetic field effect in the coincidence counting rates. That is, the effect of the changing magnetic field on the anode signals was measurably greater than its effect on the dynode signals. This difference in magnetic field sensitivity was primarily due to the β detector. In order to provide good stabilization for both the timing and energy resolution pulse, we decided to integrate the charge from the anode current pulse and stabilize from the resulting signal.

Stabilizing the photomultiplier tubes off the integrated timing signals did reduce the magnetic field sensitivity of the instrument.

However, the coincidence counting rates were still more sensitive to the magnetic field than the single counting rate from the integrated anode pulse. The persistence of larger magnetic field sensitivity for the timing signals compared to the integrated anode signal implied that the magnetic field was affecting the shape of the anode current pulse or the transit time in the photomultiplier tube but was not altering the total charge delivered at the anode.

In an effort to cancel the magnetic field in the vicinity of the β photomultiplier tube, a compensating coil wired in parallel with the magnet was tried on the β detector. A similar coil was already in use on the γ detector. However, due to the different geometries of the two detectors, the β compensating coil was not as effective as the γ compensating coil.

The final solution to the magnetic field sensitivity problem was to move the β photomultiplier tube farther away from the scattering magnet by inserting a six inch light pipe. The light pipe also permitted us to provide better magnetic shielding for the photomultiplier tube (Netic and Co-Netic foils were used). In the previous β detector configuration¹⁰ the β energy resolution was 15% FWHM for 624 keV conversion electrons. With the 6 inch light pipe the resolution was 17% .

In its final form the stabilizing system was very effective. There was no appreciable change in the gain of the β detector when the β counting rate was changed from 10^4 to 5×10^5 counts per second. The changes in β and γ single counting rates as a function of the magnetic field were typically 0.02%. The average deviations of the single counting rates were typically 0.1% .

The coincidence counting rate sensitivity was tested by replacing the usual collimators with a lead shield which permitted γ rays to go directly to the γ detector but prevented γ rays from scattering from the magnet into the γ detector. The γ detector was left in its usual position so that the effect of the magnetic field would be the same as during the experiment. With this arrangement δ was found to be consistent with zero as expected:

$$\delta = - 0.00004 \pm 0.0006 .$$

The efficiency parameters ϵ_n introduced in equation 9 were calculated with a computer using the method discussed by Schopper⁷. The accuracy of the computer program has been checked previously¹⁰ by calculating and measuring the efficiency for the γ rays following the β decay of Co^{60} . In the present experiment a larger angular spread was used at the entrance to the analyzing magnet to increase the data collection rate, so P_γ was again measured for Co^{60} to check the program for these new conditions. The result for the experimental value of ϵ_1 was

$$-3 \langle \delta / (v/c) \rangle = \epsilon_1 = - 0.0495 \pm 0.0054$$

(ϵ_1 is a negative number because it contains $\langle P_1(\theta) \rangle$.)

The calculated value of ϵ_1 was

$$\epsilon_1 = - 0.051 \pm 0.004$$

The major source of uncertainty in the calculated value of ϵ_1 comes from the uncertainty in the fraction f of polarized electrons in the

scattering magnet. [$f = (6.5 \pm 0.3)\%$] . Since there is good agreement between the experimental and calculated efficiency in the new and old geometry, the computer program can be used with confidence to calculate ϵ_n for As^{76} . The results are

$$\epsilon_1 = -0.039 \pm 0.003 \quad \epsilon_2 = 0.75 \pm 0.03 \quad \epsilon_3 = -0.023 \pm 0.0017$$

The efficiency ϵ_1 is lower for As^{76} than Co^{60} because of the lower γ ray energy of As^{76} . Since the average entrance angle to the magnet (158°) is quite different from 180° , ϵ_3 is appreciably smaller than ϵ_1 .

As^{76} was obtained weekly and a new source was prepared daily. The arsenic was dissolved in hydrochloric acid, making the isotopic form a liquid at room temperature. In order to convert the arsenic chloride into a form which would precipitate on evaporation, nitric acid was added to the radioactive solution before evaporation, and the resultant solution was concentrated by boiling. In this way arsenic pentoxide was formed which crystallized under heat evaporation. Each source was prepared by placing drops of the radioactive As_2O_5 solution onto a thin gold film which had been deposited by vacuum evaporation on $\frac{1}{4}$ -mil mylar. Then the drops were evaporated to dryness. The radioactive deposits were restricted to a $\frac{1}{4}$ inch diameter circle.

The sources prepared at the end of the week were much thicker than the sources prepared immediately after receiving fresh material. The amount of As on the source varied from 0.05 mg to 0.7 mg. Of course, sources prepared by evaporation to dryness are not uniform, so it was not possible to calculate the source thickness. However, we did not expect the source thickness to distort the data since the β

particle energy was so large. When the final results were examined, there was no statistically significant change in δ as a function of the source thickness.

During the measurements the magnetic field was reversed every 10 minutes. Even though this period is short compared to the half life of the source (26.5 hrs), it was still necessary to carefully correct for the decay of the source in order to be able to check the stability of the equipment accurately. The average strength of the source during each 10 minute measurement and the change in the true to chance coincidence ratio were included in the corrections.

During the calibration run on Co^{60} P_{γ} was measured as a function of the β particle energy in a manner identical to that described in reference 10. Observing the energy dependence as well as the magnitude of P_{γ} provides an additional check on the performance of the instrument.

A different mode of operation was used when the circular polarization correlation of As^{76} was measured. It is clear from the partial decay scheme for As^{76} shown in Figure 2 that the 1.76 MeV β transition limits the energy range for which measurements can be made on the 2.41 MeV transition. Furthermore, an analysis using the other experimental observables showed that the energy dependence of P_{γ} was likely to be small in the available energy region. Therefore, for the As^{76} measurements, a single channel analyzer was set to accept electrons in the energy interval from 1.4 to 2.0 MeV. Less than 5% of the coincidence events in this interval were due to the 1.76 MeV transition. (A second window was set from 2.0 to 2.4 MeV, but the number of events in this interval was too small to yield usable statistical accuracy for the

matrix element extraction.)

One of the major advantages of the electronic system used in the experiment is that it can collect data rapidly since it will accept very high β single counting rates (up to 10^6 counts/second). However, this capability cannot be used if the source strength is limited by the true-to-chance coincidence ratio. The true-to-chance coincidence ratio is low in the experiment because of the 2.97 MeV transition to the ground state. This problem was overcome by using a time to amplitude converter (TAC) to record the β - γ coincidences. The TAC output was routed to alternate halves of a multichannel analyzer by the magnet control system. The number of true coincidences could be accurately determined by using the complete TAC spectrum to correct for the chance coincidence events. The full width at half maximum of the true coincidence peak was 3.7 nsec.

The following result was obtained for the circular polarization parameter δ :

$$\delta = 0.0041 \pm 0.0008$$

for $1.4 \text{ MeV} < E_{\beta} < 2.0 \text{ MeV}$, $\langle \theta_{\beta\gamma} \rangle = 158^{\circ}$. The uncertainty is primarily statistical with a small contribution from the uncertainty in the efficiency.

III. Matrix Element Extraction

The following data was used to set limits on the nuclear matrix elements: the circular polarization obtained in the present experiment, the β - γ directional correlation of Fischbeck and Newsome¹¹

and Raghavan, Grabowski, and Steffen¹², the nuclear orientation results of Pipkin, Bradley, and Simpson¹³, and the β spectrum shape of Nagarajan¹⁴. This experimental data is not adequate to give an unambiguous set of nuclear matrix elements. Therefore, in the following presentation of the results, theoretical arguments are given which show that one type of solution is much more likely to be correct than the other possibilities.

The details of the matrix element extraction have been published previously^{2,6}. Exact electron radial wave functions were used¹⁵, and the effect of screening by atomic electrons was included¹⁶. The most distinctive feature of the analysis is the procedure used to include higher order matrix elements. The most important higher order matrix element parameters are x' and u' because these parameters occur in Y with a relatively large coefficient ($d = -0.185$, see Table 1). The parameter λ which occurs in the theoretical expression for the vector matrix element ratio Λ_{CVC} (Equation 2) is equal to x'/x . Therefore, a restriction can be placed on the higher order matrix element x' by requiring that the experimental value Λ_{exp} and the theoretical value Λ_{CVC} of the vector matrix element ratio agree.

$$\Lambda_{exp} = D'y_0/x$$

Requiring agreement with the Damgaard and Winther value for Λ_{CVC} is very different from requiring agreement with the Fujita-Eichler value for Λ_{CVC}^0 . Fujita and Eichler assumed that the Coulomb hamiltonian was diagonal. The procedure used here makes no assumption about the contribution of the off diagonal elements of the Coulomb hamiltonian.

The only restriction is that the contribution be the same in Λ_{CVC} and in the β observables.

A complete derivation for Λ_{CVC} is given in reference 6. The CVC theory has been tested experimentally so the primary question about the derivation is whether or not the assumed form of the Coulomb potential is adequate. Fayans and Khodel have discussed the effect on the Coulomb potential of including quasi-particle interactions. In their first paper¹⁷ they suggested that the potential used by Damgaard and Winther was not adequate. However, after including further refinements, these authors later concluded¹⁸ that the simple potential used by Damgaard and Winther was correct.

There is also experimental evidence¹⁹ from an analysis of Rb⁸⁶ for the validity of the Damgaard and Winther expression for Λ_{CVC} . When the value of λ was adjusted so that some acceptable matrix element sets had Λ_{exp} equal to Λ_{CVC} , then the experimental data excluded any set of matrix elements for which Λ_{exp} and Λ_{CVC} did not agree to within 20%. This agreement between Λ_{exp} and Λ_{CVC} occurred for reasonable values of λ ($-0.6 < \lambda < 0.8$).

In the present analysis of As⁷⁶ the existing experimental data is not sufficient to set good limits of error on the matrix elements. Therefore, we have analyzed the data using the restriction that Λ_{exp} must agree with Λ_{CVC} to within 20%. This restriction seems quite reasonable considering the theoretical and experimental evidence for the Damgaard and Winther expression for Λ_{CVC} .

The operators in the matrix elements u and x and in u' and x' have the same radial dependence. Thus it is reasonable to expect that

u'/u will have approximately the same value as x'/x .

$$u'/u \approx x'/x = \lambda$$

With this assumption the parameter λ can also be used to make an accurate estimate of the contribution of u' to the β decay.

The contribution of the higher order parameters y' , w' , and z' is less important because they enter the formulas with a small coefficient ($a = -0.029$). Nevertheless, the results are quoted for y_0 , w_0 , and z_0 not y , w , and z to make clear that there are small contributions from y' , w' , and z' . In unusual cases the distinction between y_0 and y could be important. The experimental value of the vector matrix element ratio is $\Lambda_{\text{exp}} = D'y_0/x$, and the theoretical value is $\Lambda_{\text{CVC}} = D'y/x$. If it is possible for y' to be much larger than y , then it is difficult to compare Λ_{exp} and Λ_{CVC} . The higher order parameters s' , r' , and t' have even smaller coefficients so they are completely neglected.

In summary, the procedure is to vary λ and accept all sets of matrix elements which agree with the experimental data and have a value of Λ_{exp} which agrees with Λ_{CVC} to within 20%. The experimental data places a restriction on the range over which λ must be varied.

If λ is outside the range -2 to +3, Λ_{exp} does not agree with Λ_{CVC} for As^{76} .

In order to demonstrate the improvement that can be made by using Λ_{CVC} , the analysis was performed with and without a restriction on Λ_{exp} . Three typical sets of matrix element parameters are shown in Table 2. In each of the sets, the contribution of the higher order matrix elements was assumed to be $x'/x = u'/u = 0.6$. The theoretical

value of Λ_{CVC} is 0.34 when $\lambda = 0.6$. Λ_{exp} for set 1 is in good agreement with Λ_{CVC} , while for sets 2 and 3 Λ_{exp} is much too low. There is a second reason for rejecting sets similar to 2 and 3. In both cases w_0 is much greater than V . Even though it is possible for w and v to cancel so that the combination V is smaller than the individual matrix elements, such a large cancellation in V is very unlikely.

A more complete picture of the effect of using Λ_{CVC} is shown in Table 3. The definition of the parameters is given in Table 1. Limits of uncertainty on the matrix elements are shown with a 20% restriction on Λ_{exp} and with no restriction on Λ_{exp} . When Λ_{CVC} is used the limits are valid for all acceptable values of λ . However, when Λ_{CVC} was not used the contribution of x' and u' was fixed at 0.6. The uncertainties for the analysis without Λ_{CVC} would have been even larger if the contribution of x' and u' had been varied.

The advantages of using Λ_{CVC} in the analysis are evident. Much better limits can be set on the matrix elements, the most important higher order matrix elements x' and u' can be included in the analysis, and additional nuclear structure information can be obtained by setting limits on the ratio λ of two of the radial matrix elements.

IV. DISCUSSION

In order to interpret the results presented in Table 3, it is important to recognize that there is a strong correlation among the matrix elements. The true value for a particular matrix element may be anywhere within the range of uncertainty quoted. However, when one matrix element is fixed at a particular value, the experimental data

would usually set limits of uncertainty on the other matrix elements which would be much smaller than the limits given here. Therefore, when a nuclear model is tested, it is not sufficient that the theoretical matrix elements lie within the quoted limits. The theoretical matrix elements must predict observables which are consistent with the experimental data.

As a further example of the interplay among the matrix elements, it is not necessarily valid to assume that the matrix element ηz_0 has the maximum size its limits permit while all of the other matrix elements have their minimum possible sizes.

The most probable value of a matrix element is the value which occurs most frequently in the analysis. (This argument has been presented in detail in reference 2). The most probable values when Λ_{exp} is restricted are given in Table 3. The normalization is such that the maximum physical size of a radial matrix element is $\sqrt{2}$. The maximum expected size of a relativistic matrix element is approximately a factor of 10 smaller. All of the matrix elements of As^{76} are reduced by an order of magnitude from their maximum possible size. The contribution of the $\Delta J = 0, 1, \text{ and } 2$ matrix elements are approximately equal. This result is not even in qualitative agreement with the general prediction of the shell model that the B_{ij} matrix element (ηz) will be dominant in nonunique first forbidden transitions. As is usually the case, the data cannot set good limits on ηw_0 because the experimental observables are insensitive to this parameter.

When the matrix elements must be in a very restricted range in order to make Λ_{exp} and Λ_{CVC} agree for a particular value of λ ,

then that λ is not likely to be the true value. When there is a different λ for which Λ_{exp} and Λ_{CVC} agree for a large range of matrix elements, one of these matrix element sets is likely to be the correct set. Therefore, the most probable value of λ is taken as the point where agreement between Λ_{exp} and Λ_{CVC} is least sensitive to the exact size of the matrix elements. The result of $\lambda = 0.8$ indicates that the contribution of the off diagonal matrix elements of the Coulomb hamiltonian is small. However, a large contribution cannot be excluded.

As was noted in the introduction, the circular polarization P_{γ} cannot be determined from the observed effect δ unless the correlation coefficients A_1 , A_2 , and A_3 are known. A_2 is known experimentally. In all of the sets which met the restriction on Λ_{exp} , A_1 was much larger than A_3 . Therefore, A_3 was set equal to zero, and P_{γ} was determined from δ by using equations 7 and 9.

$$P_{\gamma}(1.4 \text{ MeV} < E_{\beta} < 2.0 \text{ MeV}, \theta_{\beta\gamma} = 180^{\circ}) = + 0.105 \pm 0.02$$

The analysis also shows the importance of using δ rather than P_{γ} in the matrix element extraction. Sets similar to 2 and 3 in Table 2 frequently had values of A_3 which were larger than A_1 . For such a set, the P_{γ} consistent with δ would be larger because ϵ_3 is less than ϵ_1 .

We have also investigated the possibility of performing additional experiments which could set better limits of error on the matrix elements and also confirm the theoretical predictions which have been used in the present analysis. The two experimental observables which would be most useful are the beta spectrum shape correction factor $C(W)$ and the

β energy dependence of P_γ . The theoretical values of $P_\gamma(W)$ and $C(W)$ for sets 2 and 3 are different from the theoretical values for set 1. However, it would be quite difficult to obtain sufficient experimental accuracy to distinguish between the sets. $C(W)$ would have to be measured with at least 1.5% accuracy in the energy interval from $E_\beta = 1.7$ MeV to 2.2 MeV, or $C(W)$ would have to be measured with at least 2.5% accuracy from $E_\beta = 1.0$ MeV to 2.2 MeV. In order to measure $P_\gamma(W)$ with sufficient accuracy it would take approximately one year with our instrument which accumulates data very rapidly. Unfortunately, neither measurement would confirm the theoretical prediction that Λ_{exp} must be approximately equal to Λ_{CVC} . Since there are two good theoretical reasons for excluding sets similar to 2 and 3, further measurements on $C(W)$ and $P_\gamma(W)$ do not appear to be worthwhile. The nuclear matrix elements are even less sensitive to the nuclear orientation and β - γ directional correlation parameters, so there appear to be no additional experiments which would really be useful.

The authors would like to express their appreciation to Mr. J. S. Schweitzer for his assistance in the matrix element analysis.

FIGURE CAPTIONS

1. Schematic diagram of the detector and scattering magnet geometry.
2. Partial decay scheme for As^{76} .

REFERENCES

† Work supported in part by the United States Atomic Energy Commission under Contract AT(11-1)1746.

* Present address: Los Alamos Scientific Laboratory, Los Alamos, New Mexico 87544.

1. W. Buhring, Nucl. Phys. 40 (1963), 472.
2. P. C. Simms, Phys. Rev. 138 (1965), B784.
3. J. I. Fujita, Phys. Rev. 126 (1962), 202.
4. J. Eichler, Z. Phys. 171 (1962), 463.
5. J. Damgaard and A. Winther, Phys. Lett. 23 (1966), 345.
6. H. A. Smith and P. C. Simms, Phys. Rev. 1C (1970), 1809.
7. H. Schopper, Nucl. Instr. 3 (1958), 158.
8. K. Siegbahn, ed., Alpha-, Beta-, and Gamma-Ray Spectroscopy, North-Holland Publishing Co., Amsterdam (1966), Ch. XXIV-G.
9. P. Alexander, Ph.D. Thesis, Purdue University, 1961.
10. D. E. Ohlms, J. J. Bosken and P. C. Simms, Phys. Rev. 1C (1970), 1803.
11. H. J. Fischbeck and R. W. Newsome, Phys. Rev. 129 (1963), 2231.
12. R. S. Raghavan, et. al., Phys. Rev. 139 (1965), B1.
13. F. M. Pipkin, et. al., Nucl. Phys. 27 (1961), 353.
14. T. Nagarajan, Nucl. Phys. A137 (1969), 467.
15. C. P. Bhalla and M. E. Rose, Oak Ridge National Laboratory Report No. ORNL-3207 (unpublished).
16. W. Buhring, Nucl. Phys. 61, 110 (1965).
17. S. A. Fayans and V. A. Khodel, Phys. Letters 30B (1969) 5.
18. S. A. Fayans and V. A. Khodel, Phys. Letters 31B (1969) 99.
19. J. J. Bosken, D. E. Ohlms, P. C. Simms, Phys. Rev. C3, (1971).

Table 1. Definition of Matrix Element Parameters

For $\Delta J = 0$

$$DV = D'v_0 + D(w + dw')$$

$$D'v = \frac{C_A}{\eta} \int \gamma_5$$

$$w = -\frac{C_A}{\eta} \int i \frac{\vec{\sigma} \cdot \vec{r}}{\rho}$$

$$w' = -\frac{C_A}{\eta} \int i \frac{\vec{\sigma} \cdot \vec{r}}{\rho} \left(\frac{r}{\rho}\right)^2$$

$$w_0 = \frac{w + \frac{3}{5} a w'}{1 + a}$$

For $\Delta J = 1$

$$DY = D'y_0 - D[(x + dx') + (u + du')]$$

$$D'y = \frac{C_V}{\eta} \int \vec{\alpha}$$

$$D'y = \frac{C_V}{\eta} \int \vec{\alpha} \left(\frac{r}{\rho}\right)^2$$

$$y_0 = \frac{y + ay'}{1 + a}$$

$$x = \frac{C_V}{\eta} \int i \frac{\vec{r}}{\rho}$$

Table 1. (contd.)

$$x' = \frac{C_V}{\eta} \int i \frac{\vec{r}}{\rho} \left(\frac{r}{\rho} \right)^2$$

$$u = \frac{C_A}{\eta} \int \frac{\vec{\sigma} \times \vec{r}}{\rho}$$

$$u' = \frac{C_A}{\eta} \int \frac{\vec{\sigma} \times \vec{r}}{\rho} \left(\frac{r}{\rho} \right)^2$$

For $\Delta J = 2$

$$z = -\frac{C_A}{\eta} \int i \frac{B_{ij}}{\rho}$$

$$z' = -\frac{C_A}{\eta} \int i \frac{B_{ij}}{\rho} \left(\frac{r}{\rho} \right)^2$$

$$z_0 = \frac{z + \frac{4}{5} az'}{1 + \frac{4}{5} a}$$

$$D = \frac{1}{2} \alpha Z + W_0 \rho$$

$$d = -\frac{1}{5D} \left[\frac{\alpha Z}{2} - a(3D + \frac{2}{3} q\rho) \right]$$

$$a = -\frac{1}{6} \left[(W_0 + \frac{3}{2} \alpha Z)^2 - \rho^2 \right]$$

where $Z = \pm |Z|$ for β^\mp decay

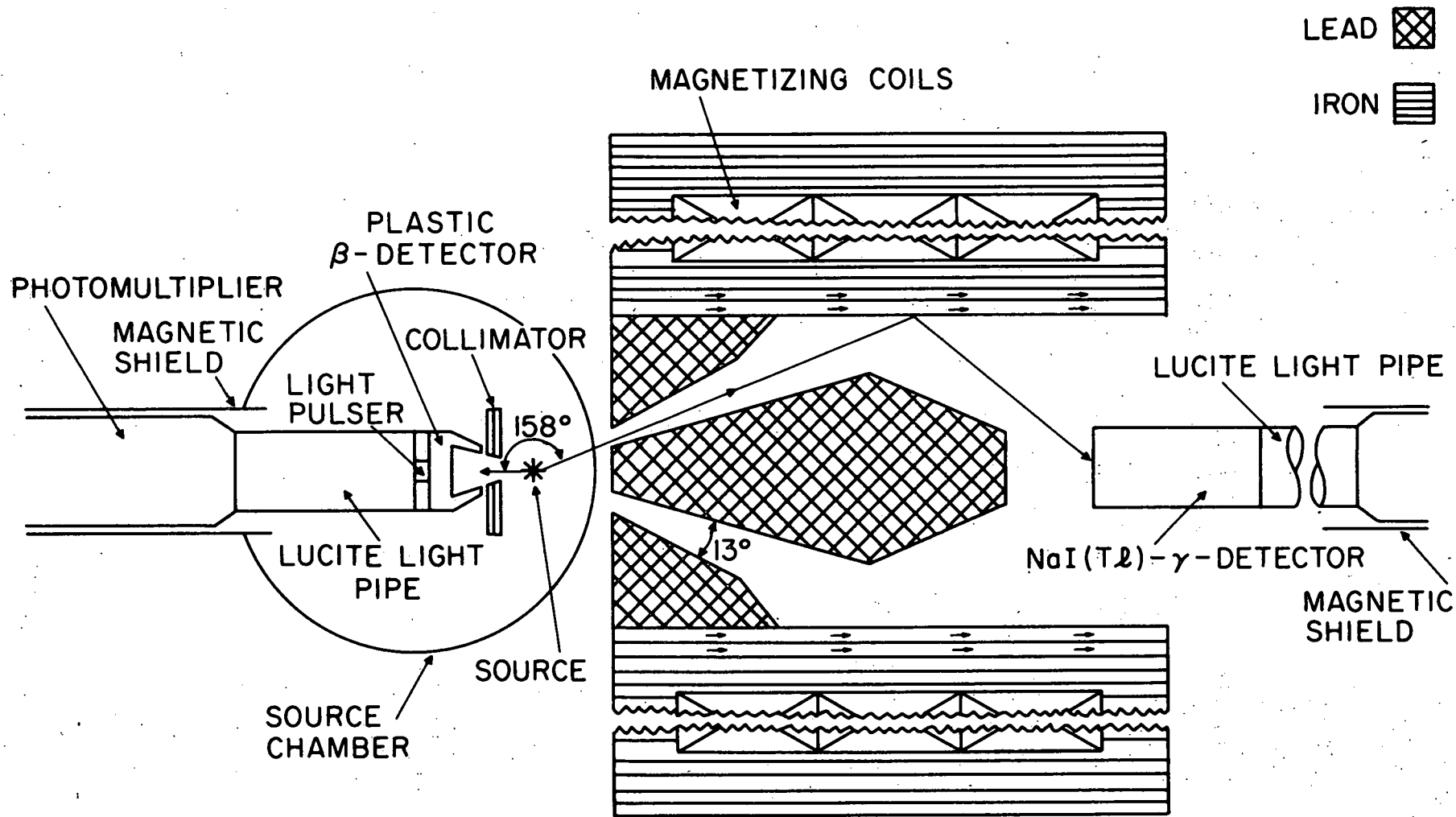
Table 2. Typical matrix element parameter sets.

Set	$\Delta J = 0$		$\Delta J = 1$				$\Delta J = 2$	λ	Λ_{exp}
	V	w_o	Y	$D'y_o$	x	u	z_o		
1	-0.622	-2.86	-0.266	-0.176	-0.577	-0.433	1.0	0.6	.31
2	0.0706	-12.0	0.284	0.0526	0.297	-0.220	1.0	0.6	.18
3	-1.31	42.1	0.979	0.647	4.87	-1.16	1.0	0.6	.13

Table 3. Results for the nuclear matrix elements of the 2.41 MeV transition in As^{76} . The definition of the parameter is given in Tabel 1.

$$D = 0.149 \quad d = -0.185 \quad a = -0.029 \quad \rho = 0.0129$$

Matrix Elements	Results with $\Lambda_{exp} = \Lambda_{CVC} \pm 20\%$	Results without using Λ_{CVC}
η_V	+ 0.007 -0.04 - 0.001	-0.01 \pm .035
η_{w_0}	0 \pm 0.3	0 \pm 1
η_X	+ 0.018 -0.017 - 0.011	0 \pm 0.03
$\eta_{D'y_0}$	+ 0.008 -0.012 - 0.010	0 \pm 0.025
η_x	+ 0.025 -0.038 - 0.017	0.02 \pm 0.075
η_u	+ 0.052 -0.028 - 0.064	-0.036 \pm 0.07
η_{z_0}	+ 0.030 +0.065 - 0.010	0.073 \pm 0.06
λ	+ 2.2 0.8 - 2.8	



1 INCH

